Electronic Supplementary Material (ESI) for Lab on a Chip.

Supplementary Information for

Blood Platelet Enrichment in Mass-producible Surface Acoustic Wave (SAW) driven Microfluidic Chips

Cynthia Richard, Armaghan Fakhfouri, Melanie Colditz, Friedrich Striggow, Romy Kronstein-Wiedemann, Torsten Tonn, Mariana Medina-Sánchez, Thomas Gemming, Andreas Winkler

Andreas Winkler.
E-mail: a.winkler@ifw-dresden.de

This PDF file includes:

Figs. S1 to S6
Table S1
Captions for Movies S1 to S5
References for SI reference citations

Other supplementary materials for this manuscript include the following:

Movies S1 to S5

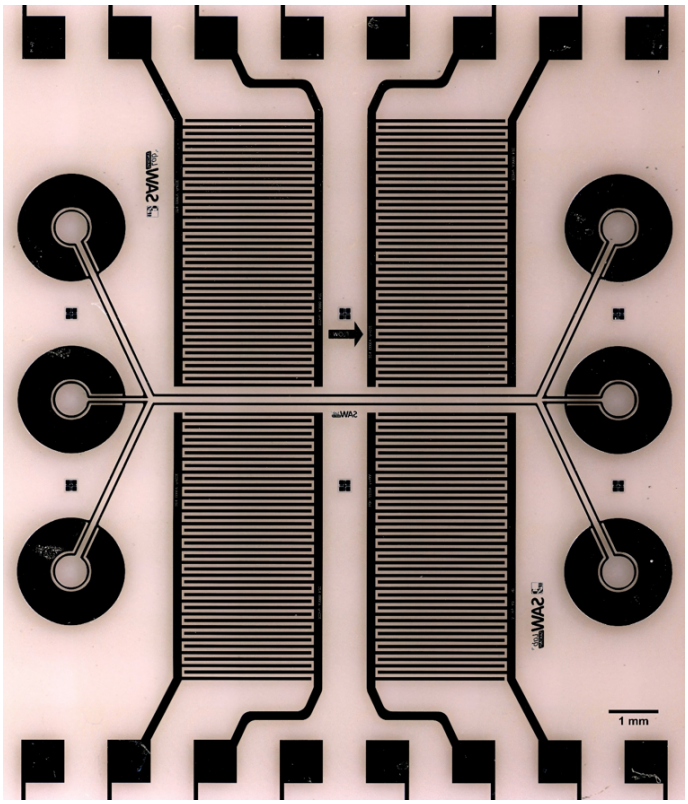

Fig. S1. Optical microscope image of the chip layout used in the experiment.

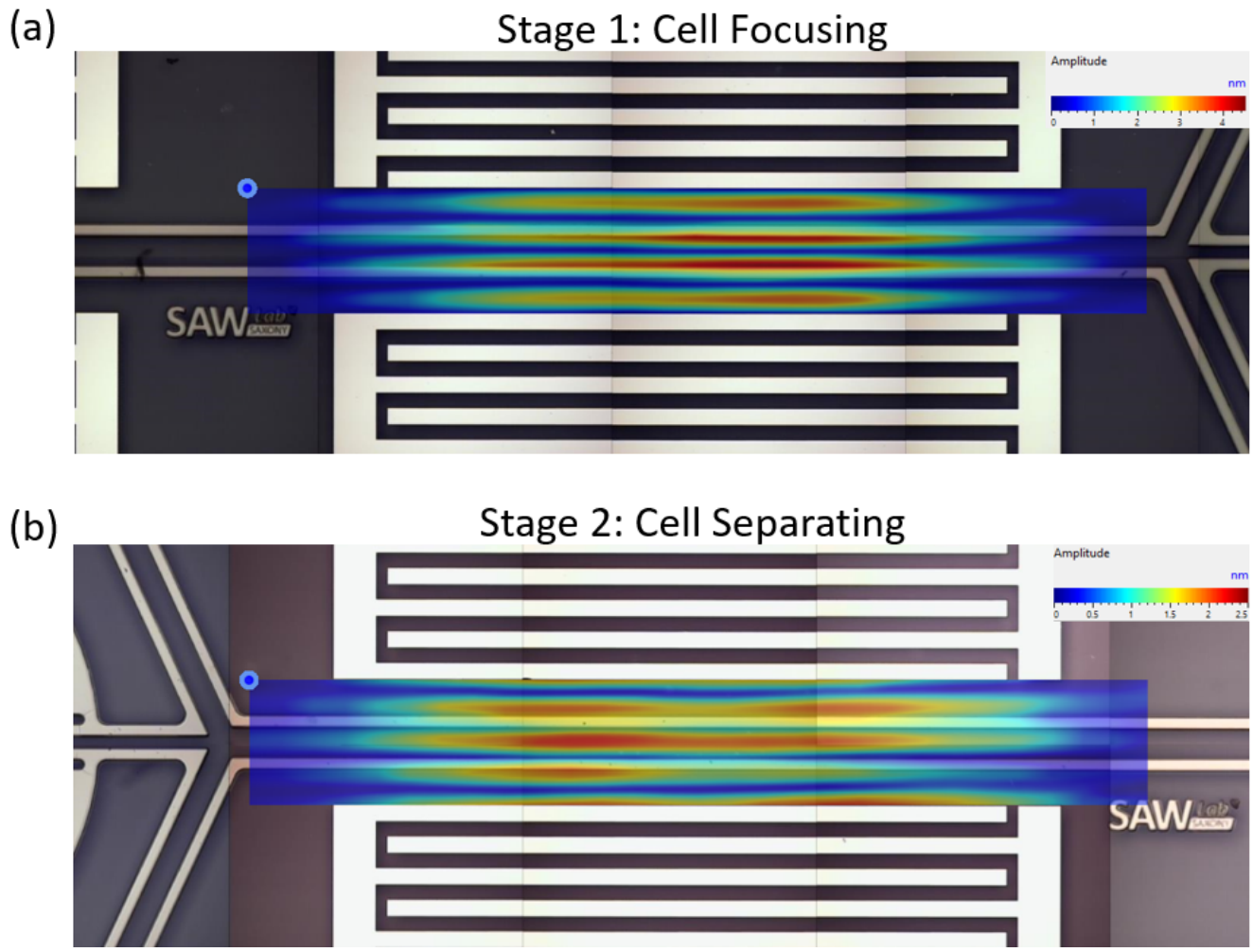

Fig. S2. High frequency laser-Doppler vibrometry measurements showing the amplitude of the standing wave field excited on the chip surface. (a) The focusing stage of the device excited at 13 MHz with an applied power of 150 mW where a pressure node (blue) is seen in the channel center. The maximum displacement amplitude at the nodal region inside the channel was measured to be 3.3 nm, and 4 nm outside of the channel. (b) The separating stage of the device excited at 12.7 MHz with an applied power of 120 mW where a pressure anti-node (red) is seen in the channel center with two regions of low pressure amplitude at the channel walls. The maximum displacement amplitude at the nodal region inside the channel was measured to be 1.5 nm, and 2 nm outside of the channel.

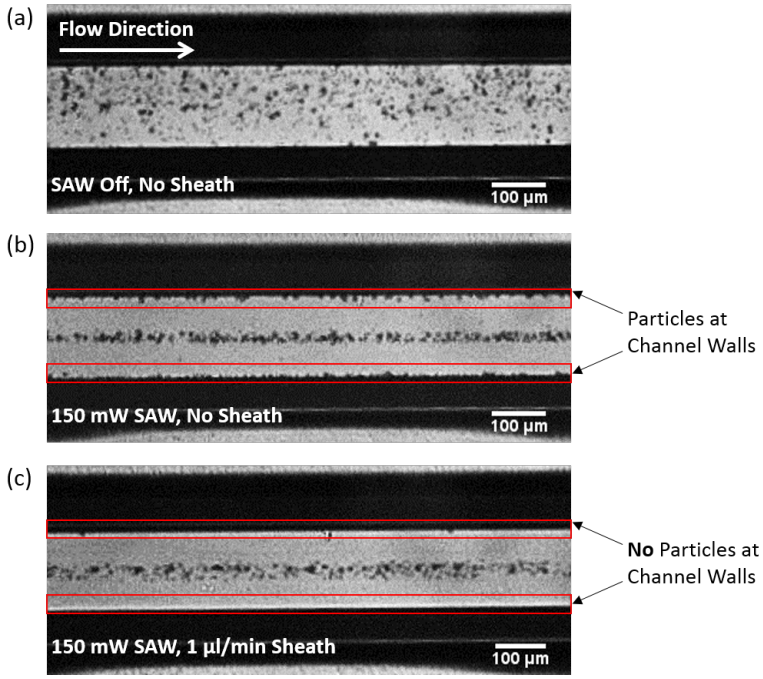

Fig. S3. Sheath flow experiments using 3 μm and 7 μm polystyrene (PS) particles. (a) Particles flowing in the microchannel at 1 μl/min with no applied SAW or sheath flow. (b) 150 mW of SAW is applied in the focusing stage of the device with no sheath flow. It can be seen that the particles become trapped in 3 nodes, one in the center of the channel as desired, as well as in 2 nodes at the channel walls which is undesired. (c) 150 mW of SAW is applied with a 0.5 μl/min sheath flow. Particles are no longer observed at the channel walls.

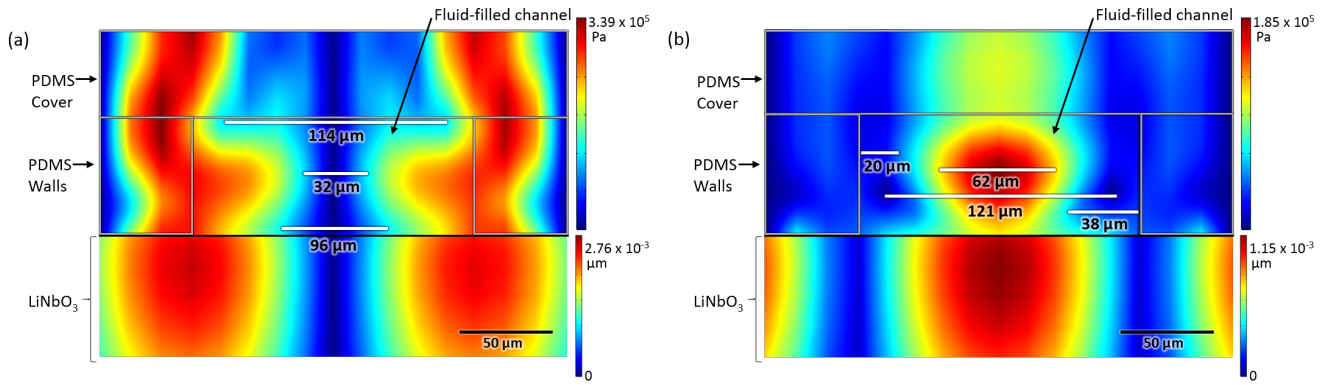

Fig. S4. FEM simulation demonstrating the acoustic field in a PDMS microchannel. The simulations show the pressure node system created inside of the microfluidic channel at the desired resonant frequency for the focusing stage (a) and the separation stage (b). Measurements of the pressure node widths are also shown for comparison to the SU-8 simulations. The scale bar shows the time-averaged absolute pressure field (<|p|>) in Pa and the absolute displacement (<|w|>) in the steady-state in μm.

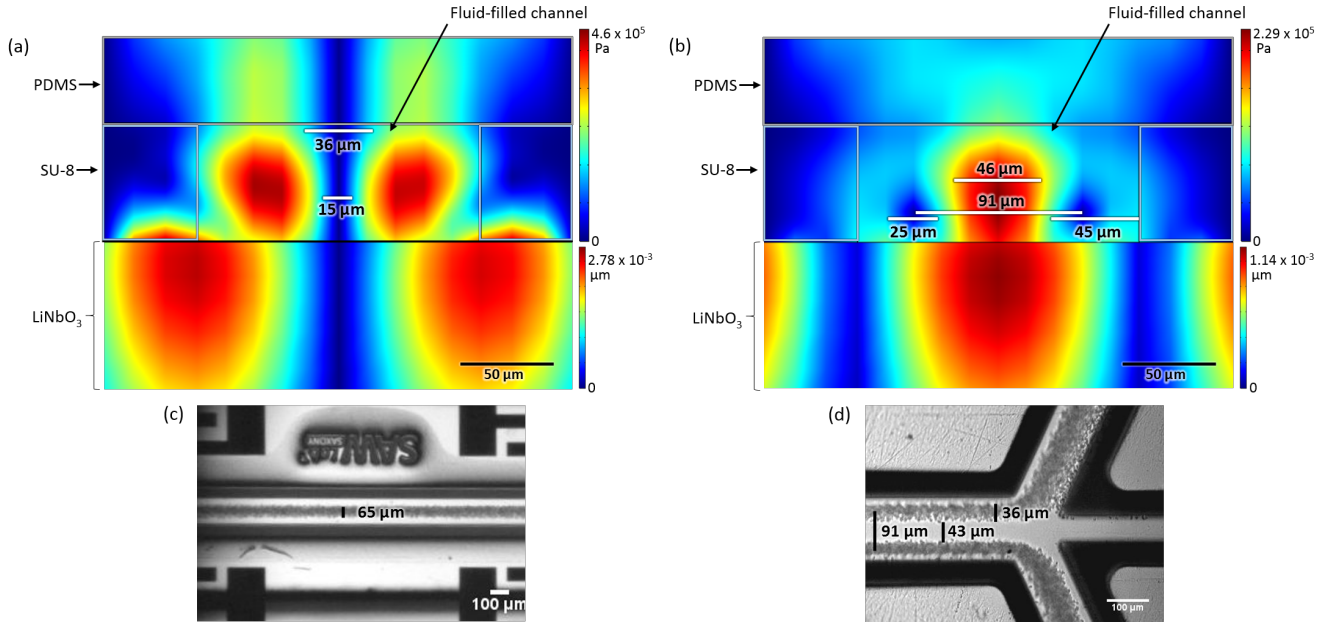

Fig. S5. Simulation of the pressure nodes with measured widths, (a) & (b), compared to the width of the blood stream during experimentation, (c) & (d). The scale bar shows the time-averaged absolute pressure field (<|p|>) in Pa and the absolute displacement (<|w|>) in the steady-state in μm.

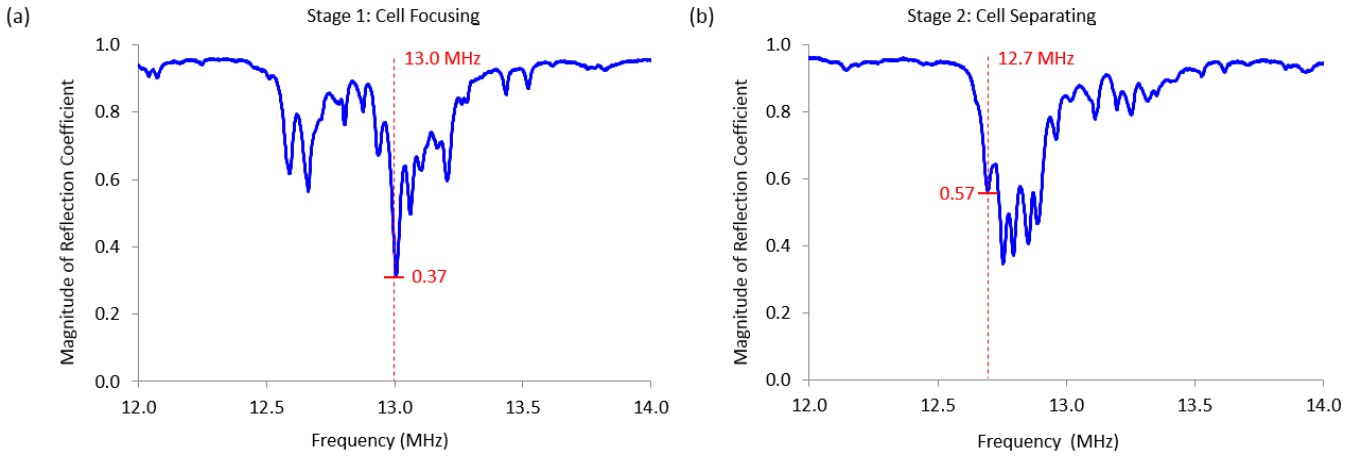

Fig. S6. Electrical network analyzer measurements of the reflection coefficient of the IDT pairs attached to splitters. (a) The resonance peak of the first pair of IDTs used for SAW focusing. A frequency of 13 MHz was used for the experiments. (b) The resonance peak of the second pair of IDTs used for SAW separation. A frequency of 12.7 MHz was used for the experiments.

Table S1. Parameters Used in COMSOL Simulation

SAW Actuation		
SAW wavelength	λ_{SAW}	300 μm
Excitation frequency:		
for focusing (180° phase)	f_{180}	13.0 MHz
for separating (0° phase)	f_0	12.7 MHz
Displacement amplitude:		
for focusing (180° phase)	d_{180}	2.75 nm
for separating (0° phase)	d_0	1.75 nm
Voltage potential:		
for focusing (180° phase)	V_{180}	68.5 V
for separating (0° phase)	V_0	43.5 V
Lithium Niobate (128° YX-cut $LiNbO_3$)		
Speed of sound (1)	C_{LN}	3994 m s^{-1}
Density (1)	ρ_{LN}	4700 kg m^{-3}
SU-8 Photoresist		
Speed of sound	C_{SU8}	2909 m s^{-1}
Density	ρ_{SU8}	1233 kg m^{-3}
Polydimethylsiloxane (PDMS; 10 : 1)		
Speed of sound (2)	C_{PDMS}	1076.5 m s^{-1}
Density (1)	ρ_{PDMS}	970 kg m^{-3}
Water		
Speed of sound (3)	C_W	1497 m s^{-1}
Density (3)	ρ_W	997 kg m^{-3}
Polystyrene		
Speed of Sound (4)	C_{PS}	2350 m s^{-1}
Density (4)	ρ_{PS}	1050 kg m^{-3}

Movie S1. Cells flowing through all three outlets with no applied SAW. This movie corresponds to Fig. 3(a). Flow is from left to right.

Movie S2. SSAW cell separation. This movie corresponds to Fig. 3(b). The red blood cells become trapped in pressure nodes created near the channel walls and are collected at the corresponding side outlets. Platelets remain in the central flow region and are collected at the central outlet. Flow is from left to right.

Movie S3. SSAW focusing and separation. This movie corresponds to Fig. 3(c). An overview of the cell focusing and cell separation is seen in the middle of the chip. Flow is from left to right.

Movie S4. Real time movie of the blood cell separation.

Movie S5. (Focusing stage) Simulation showing the pressure field development inside of the microfluidic channel over time for the focusing stage of the device where a 180° phase shift is present between the SAWs. (Separating stage) Simulation showing the pressure field development inside of the microfluidic channel over time for the separating stage of the device where no phase shift is present between the SAWs.

References

1. Fakhfouri A, et al. (2018) Surface acoustic wave diffraction driven mechanisms in microfluidic systems. *Lab Chip* 18(15):2214–2224.
2. Tsou JK, Liu J, Barakat AI, Insana MF (2008) Role of ultrasonic shear rate estimation errors in assessing inflammatory response and vascular risk. *Ultrasound Med Biol* 34(6):963 – 972.
3. Haynes W (2015) *CRC Handbook of Chemistry and Physics, 96th Edition*, 100 Key Points. (CRC Press).
4. Muller, Peter Barkholt BRJMJH, Bruus H (2012) A numerical study of microparticle acoustophoresis driven by acoustic radiation forces and streaming-induced drag forces. *Lab on a chip* 12(22):4617–4627.